

# Postannealing effects on magnetic properties and microstructure of CoCrPt/Ti perpendicular recording media

Anup G. Roy<sup>a)</sup>

*Data Storage Systems Center, Carnegie Mellon University, Pittsburgh, Pennsylvania 15213-3890*

N. T. Nuhfer

*Department of Materials Science and Engineering, Carnegie Mellon University, Pittsburgh, Pennsylvania 15213-3890*

David E. Laughlin

*Data Storage Systems Center and Department of Materials Science and Engineering, Carnegie Mellon University, Pittsburgh, Pennsylvania 15213-3890*

(Presented on 14 November 2002)

In this work, we investigate the postannealing effects on the magnetic and structural properties of CoCrPt perpendicular films. We observe a coercivity of 5000 Oe in the films with a 2 nm CrMn overlayer, which is about two times larger than the coercivity of similar films without a CrMn overlayer. This increment is attributed to the decoupling of grains by diffusion of CrMn from the top layer through the grain boundaries. An increase in the negative nucleation field and a decrease in intergranular exchange coupling with annealing temperatures was observed for the films with a CrMn overlayer. On the other hand, the films without a CrMn overlayer show the opposite trends except at high annealing temperature (450 °C). We observe a coercivity of  $\sim 7600$  Oe and a negative nucleation field of  $\sim 2400$  Oe for a film with a CrMn overlayer annealed at 450 °C for 5 min.

© 2003 American Institute of Physics. [DOI: 10.1063/1.1540162]

High coercivity, squareness, and negative nucleation field are very important for perpendicular magnetic recording media. The current challenge is to improve these properties. It is generally agreed that segregation of nonmagnetic elements to the boundaries of the columnar grains can lead to higher coercivity and lower media noise. Also, substrate heating and postannealing are the common practices used to improve magnetic properties for Co based longitudinal media by segregation and interdiffusion to the grain boundaries of nonmagnetic elements. By such interdiffusion both Cr or/ and Mn have been shown to increase the coercivity of Co based longitudinal media.<sup>1-4</sup> The effect of postannealing on Co based perpendicular media has yet to be investigated. This article presents the effect of Cr and Mn interdiffusion by rapid thermal postannealing (RTA) on the magnetic properties and microstructure of CoCrPt perpendicular media.

Two types of CoCrPt thin films were deposited at about 280 °C by rf diode sputtering onto heated naturally oxidized Si (111) wafers: Type I (without a CrMn layer): Si substrate\Ti (50 nm)\CoCrPt (30 nm) and type II (with a CrMn layer): Si substrate\Ti (50 nm)\CoCrPt (30 nm)\CrMn (2 nm). Postdeposition rapid thermal annealing was performed on the samples at atmospheric pressure under Ar flow. The Ar sputtering gas pressure was 5 mTorr and the base pressure was below  $5 \times 10^{-7}$  Torr. The sputtering rate was about 0.1 nm/s. The magnetic properties were measured using an alternating gradient force magnetometer and a vibrating sample magnetometer. The structure of the films was studied by  $\theta/2\theta$  scans and  $\omega$  scans (rocking curve) on a Philips X-pert Pro x-ray

diffractometer. A JEOL JEM 2000-EXII and a PHILIPS TECNAI F20 were used to study the microstructure of the films.

The  $\theta/2\theta$  scans and  $\omega$  scans were performed on the two types of deposited films to examine their texture and  $c$ -axis alignment. Both types of films have strong perpendicular texture. Rocking curve scans of the 00.2 CoCrPt peak give a full width at half maximum of  $\sim 5^\circ$  for both types of films. The  $M-H$  loops for films deposited without (type I) and with (type II) CrMn overlayers are shown in Fig. 1. The shapes of the two loops are seen to be different. From the coercive squareness and the slope of the hysteresis loops, it can be concluded that the film with the CrMn overlayer is more exchanged decoupled than the film without the CrMn overlayer. The film with CrMn overlayer has a lower saturation magnetization ( $M_s$ ) (about 13%) than the film without the CrMn layer and a coercivity ( $H_c$ ) of 5000 Oe, which is about two times higher than that of type I films. Since the degree of texture is similar in both films, the increase in coercivity is attributed to the decoupling of grains by the diffusion of CrMn from the top layer during deposition. This decoupling is also apparent from the difference of the slope of hysteresis loops for the two films. The small shoulder in the reversal of field detectable in both hysteresis loops is due to an initial nontextured layer in the CoCrPt films as detected by high-resolution transmission electron microscopy (TEM).<sup>5</sup>

Typical loops at different annealing temperatures for films without CrMn layer (type I) are shown in Fig. 2(a). Once again the loops are different. The slope ( $dM/dH$ ) at  $H_c$  became steeper with anneal temperature. However, the slope decreases for the loop of 450 °C. The coercivity and negative nucleation field decrease with annealing temperatures up to 400 °C and then they increase slightly at 450 °C, as shown in

<sup>a)</sup>Electronic mail: agray@ece.cmu.edu

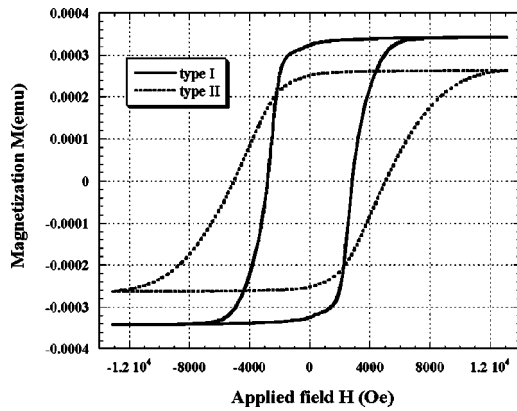


FIG. 1. Hysteresis loops for type I (without CrMn) and type II (with CrMn) as-deposited films.

Fig. 2(c). The degradation of the magnetic properties may be due to a decrease in the density of defects and faults in the film due to annealing, though this needs further investigation. The slight improvement at 450 °C is attributed to segregation of Cr to the grain boundary which contributes to decrease the exchange coupling between grains. Typical loops for type II films (with a CrMn layer) at different anneal temperatures are shown in Fig. 2(b). The loops for type II film show the opposite trend than that of type I films. The loops became more and more slanted with increasing annealing temperatures. The coercivity and the negative nucleation field increase monotonously with annealing temperature for type II films [Fig. 2(c)]. ( $H_c$  and  $-H_n$  values should be higher than the measured value since the saturation field cannot be reached for the films annealed at 400 and 450 °C due to the field limitation of the apparatus.) The improvement of the magnetic properties is due to the interdiffusion of Cr and Mn into the grain boundaries of the CoCrPt layer from the top layer as discussed later.

The exchange coupling in the film can be qualitatively understood from the differences of the value of switching volume ( $V^*$ ).  $V^*$  can be evaluated by the measurement of the dependence of the  $H_c$  on the sweep rate of the applied field.<sup>6</sup> Since the presence of the demagnetizing field causes the internal field to change following the variation of the magnetization during the measurement, the measurement of the variation of the magnetization with time in the presence of a steady negative field (time decay method) to determine the  $H_c$  cannot be applied to the films with perpendicular anisotropy.<sup>7</sup> Here we have measured the coercivities with various sweep rates (13–1300 Oe/s) to determine the  $V^*$  for the two different types of films. The plots for type I and type II films at different annealing temperatures are shown in Figs. 3(a) and 3(b), respectively. As seen from the figures, the  $H_c$  displays a linear relationship with the logarithm of the sweep rate. From the slope of the plot, the switching volumes can be calculated. The calculated  $V^*$  for both types of film are plotted as a function of annealing temperatures [Fig. 3(c)].  $V^*$  is an estimate of volume that is coherently changing the moment due to the applied field. The plot for type I films in Fig. 3(c) shows that the  $V^*$  value rises with annealing temperatures up to 400 °C. This indicates an increase of exchange coupling in the films with annealing time. The relatively lower  $V^*$  value for the film annealed at 450 °C indi-

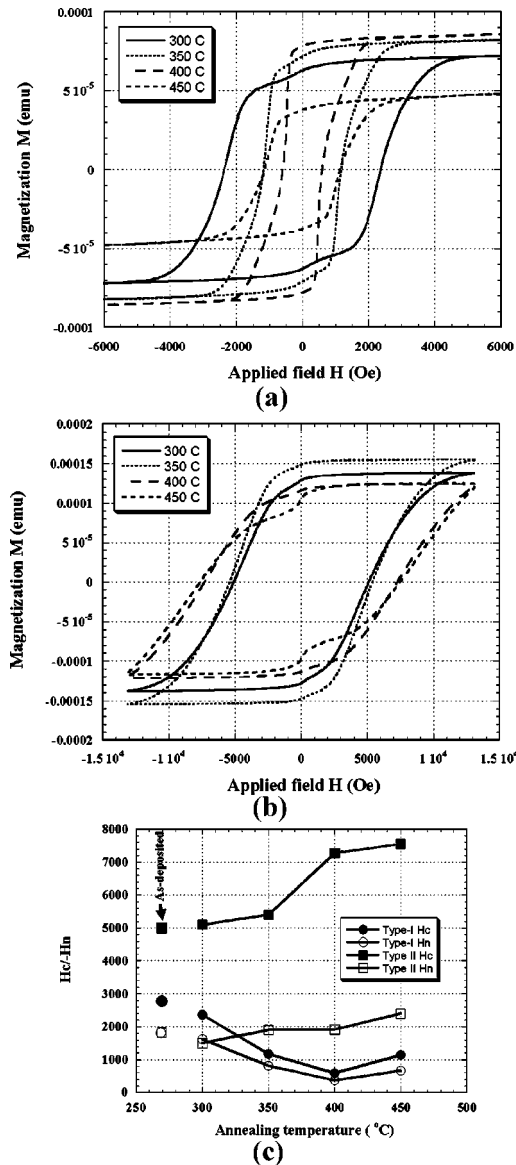


FIG. 2. (a)  $M$ - $H$  loops for type I annealed films, (b)  $M$ - $H$  loops for type II annealed films, and (c) coercivity and negative nucleation field as a function of annealing temperatures for type I and type II films (magnetization is not normalized).

cates that the film becomes relatively less exchange coupled by the segregation of Cr to the grain boundaries at this higher temperature. On the other hand, the plot for type II films shows that the  $V^*$  value falls linearly with annealing temperatures. This trend of the plot implies that the type II films become more exchanged decoupled due to diffusion of more Cr and Mn into the grain boundaries from the top layer with anneal-temperature.

To observe any microstructural changes in our film due to annealing, we have performed plan-view and cross-sectional TEM. Figures 4(a) and 4(b) show typical plan-view bright-field images of as-deposited and annealed at 450 °C type I films, respectively. Figures 4(c) and 4(d) are as-deposited and annealed at 450 °C type II films. The inset diffraction pattern for type I film shows two sets of hcp rings with  $hk.0$  rings. The set with smaller diameter is for Ti and with larger diameter is for CoCrPt films. The diffraction pattern (inset) for type II films shows two sets of hcp rings with  $hk.0$  indexing representing Ti and CoCrPt and a third set of

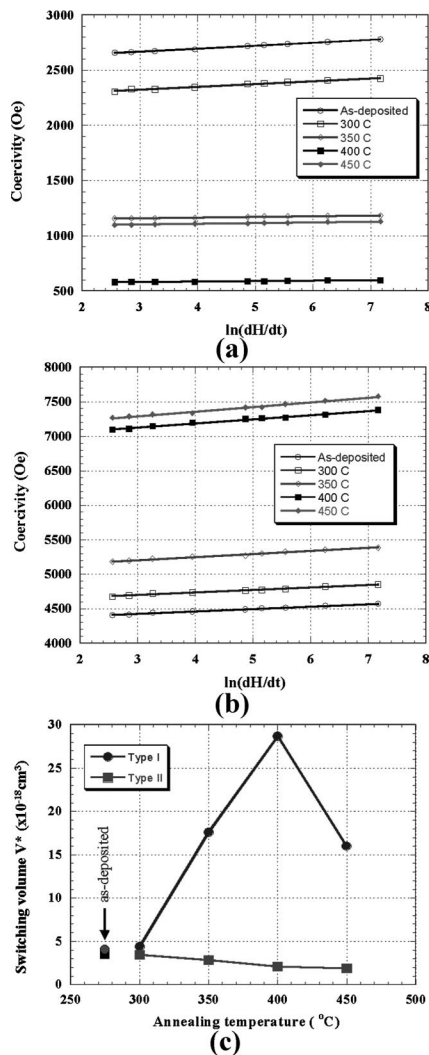


FIG. 3. (a) Coercivity dependence on the field sweep rate for type I films, (b) coercivity dependence on the field sweep rate for type II films, and (c) switching volume  $V^*$  as a function of annealing temperature for types I and II films.

bcc rings arising from the CrMn top layer. The presence of only the h $k$ .0 hcp rings in the both types of films shows that they are very strongly 00.1 textured perpendicular films. The grains of the films are small and equiaxed. Both types of the

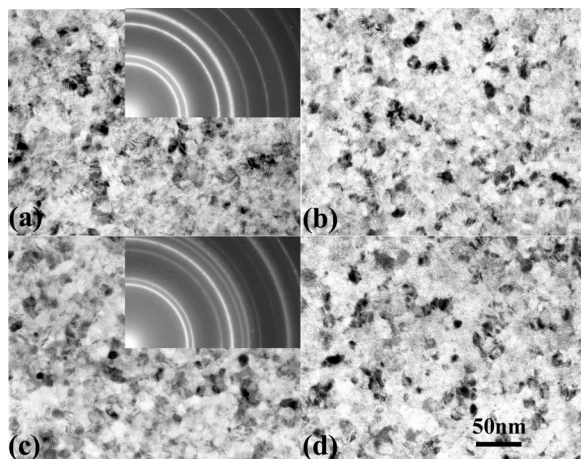


FIG. 4. Plan-view TEM bright-field images and selective area diffraction patterns: (a) type I as-deposited, (b) type I annealed at 450 °C for 5 min, (c) type II as-deposited, and (d) type II annealed at 450 °C for 5 min.

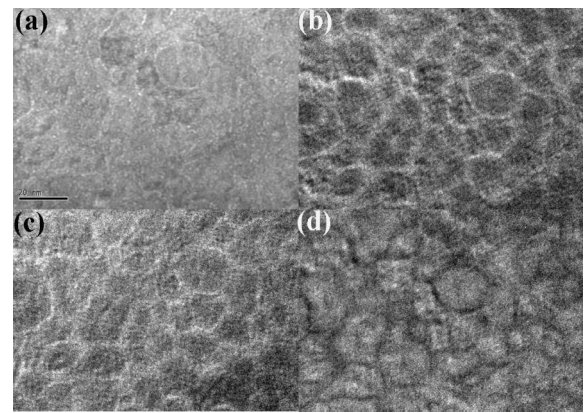


FIG. 5. Typical EELS of type II film annealed at 450 °C for 5 min: (a) is zero energy loss spectrum, (b), (c), and (d) are Cr, Mn, and Co mapping of (a), respectively. The lighter regions in (b), (c), and (d) are more enriched by Cr, Mn, and Co, respectively.

films show similar grain size. No grain growth was observed for annealed films. The mean grain size ( $\mu$ ) of both films is 12.6 nm and the standard deviation ( $\sigma$ ) of the grain size distribution is 2 nm. The similar microstructural features before and after annealing suggest that the increase in coercivity observed after annealing is due to local changes in chemistry.

To demonstrate that interdiffusion of CrMn from the overlayer into the magnetic layer occurs, the compositional distribution was examined by electron energy-loss spectroscopy (EELS). Figure 5 shows typical EELS images taken from a type II film annealed at 450 °C for 5 min. The sample for EELS observation was prepared by careful thinning from the bottom. Once the sample became electron transparent, the sample was again carefully thinned from the top to eliminate the CrMn layer, ensuring that the EELS spectrum was collected from an area that had only the CoCrPt layer present. Figure 5(a) is a zero electron energy-loss image. Figures 5(b)–5(d) are the Cr, Mn, and Co mapping of the same image. From the mapping of Cr, Mn, and Co (bright regions) it is clear that Cr and Mn do diffuse down through the grain boundaries from the top layer. This evidence clearly supports the assertion made earlier in the section that the interdiffusion of Cr and Mn into the film through the grain boundaries during annealing decoupled the grains which improves the magnetic properties.

The authors acknowledge the support of Seagate Research, Pittsburgh, PA through the Data Storage Systems Center.

- <sup>1</sup>J. Zou, D. E. Laughlin, and D. N. Lambeth, Mater. Res. Soc. Symp. Proc. **517**, 217 (1998).
- <sup>2</sup>J. Zou, B. Lu, T. Leonhardt, D. E. Laughlin, and D. N. Lambeth, J. Appl. Phys. **87**, 6869 (2000).
- <sup>3</sup>J. Jou, B. Bian, D. E. Laughlin, and D. N. Lambeth, IEEE Trans. Magn. **37**, 1471 (2001).
- <sup>4</sup>W. Peng, Z. Qian, C. Yang, J. M. Sivertson, and J. H. Judy, J. Appl. Phys. **85**, 4702 (1999).
- <sup>5</sup>A. G. Roy, S. Jeong, and D. E. Laughlin, IEEE Trans. Magn. **38**, 2018 (2002).
- <sup>6</sup>P. Bruno, G. Bayreuther, P. Beauvillan, C. Chappert, G. Lugert, D. Renard, J. Renard, and J. Seiden, J. Appl. Phys. **68**, 5759 (1990).
- <sup>7</sup>G. Bottoni, D. Candolfo, and A. Cecchetti, J. Appl. Phys. **85**, 4729 (1999).